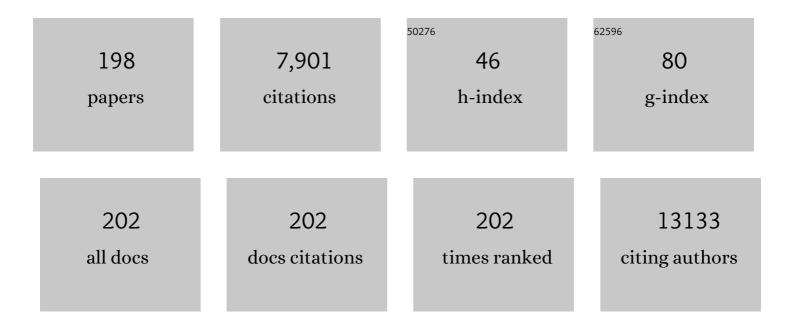
Jesus Ruiz-Cabello

List of Publications by Year in descending order

Source: https://exaly.com/author-pdf/1764070/publications.pdf Version: 2024-02-01



IESUS PULZ-CARELLO

#	Article	IF	CITATIONS
1	Neutrophils scan for activated platelets to initiate inflammation. Science, 2014, 346, 1234-1238.	12.6	516
2	Fluorine (¹⁹ F) MRS and MRI in biomedicine. NMR in Biomedicine, 2011, 24, 114-129.	2.8	429
3	Dual-Modality Monitoring of Targeted Intraarterial Delivery of Mesenchymal Stem Cells After Transient Ischemia. Stroke, 2008, 39, 1569-1574.	2.0	371
4	Mitochondrial and nuclear DNA matching shapes metabolism and healthy ageing. Nature, 2016, 535, 561-565.	27.8	333
5	Phospholipid metabolites as indicators of cancer cell function. NMR in Biomedicine, 1992, 5, 226-233.	2.8	221
6	Programmed â€~disarming' of the neutrophil proteome reduces the magnitude of inflammation. Nature Immunology, 2020, 21, 135-144.	14.5	180
7	High-b-Value Diffusion-weighted MR Imaging for Pretreatment Prediction and Early Monitoring of Tumor Response to Therapy in Mice. Radiology, 2004, 232, 685-692.	7.3	155
8	In vivo "hot spot―MR imaging of neural stem cells using fluorinated nanoparticles. Magnetic Resonance in Medicine, 2008, 60, 1506-1511.	3.0	143
9	High-resolution MRI detects cartilage swelling at the early stages of experimental osteoarthritis. Osteoarthritis and Cartilage, 2001, 9, 463-472.	1.3	141
10	Na+ controls hypoxic signalling by the mitochondrial respiratory chain. Nature, 2020, 586, 287-291.	27.8	139
11	Stress-Induced Depressive Behaviors Require a Functional NLRP3 Inflammasome. Molecular Neurobiology, 2016, 53, 4874-4882.	4.0	134
12	Helium-3 MRI diffusion coefficient: correlation to morphometry in a model of mild emphysema. European Respiratory Journal, 2003, 22, 14-19.	6.7	128
13	Fe-based nanoparticulate metallic alloys as contrast agents for magnetic resonance imaging. Biomaterials, 2005, 26, 5695-5703.	11.4	115
14	Probiotics Prevent Dysbiosis and the Rise in Blood Pressure in Genetic Hypertension: Role of Short hain Fatty Acids. Molecular Nutrition and Food Research, 2020, 64, e1900616.	3.3	113
15	NLRP3 inflammasome suppression improves longevity and prevents cardiac aging in male mice. Aging Cell, 2020, 19, e13050.	6.7	111
16	Myocardial VHL-HIF Signaling Controls an Embryonic Metabolic Switch Essential for Cardiac Maturation. Developmental Cell, 2016, 39, 724-739.	7.0	106
17	Contrast agents for MRI based on iron oxide nanoparticles prepared by laser pyrolysis. Journal of Magnetism and Magnetic Materials, 2003, 266, 102-109.	2.3	105
18	Exercise Triggers ARVC Phenotype in Mice Expressing a Disease-Causing Mutated Version of Human Plakophilin-2. Journal of the American College of Cardiology, 2015, 65, 1438-1450.	2.8	104

#	Article	IF	CITATIONS
19	Fluorocapsules for Improved Function, Immunoprotection, and Visualization of Cellular Therapeutics with MR, US, and CT Imaging. Radiology, 2011, 258, 182-191.	7.3	100
20	Gene expression profiling reveals early cellular responses to intracellular magnetic labeling with superparamagnetic iron oxide nanoparticles. Magnetic Resonance in Medicine, 2010, 63, 1031-1043.	3.0	99
21	In Vivo proton spectroscopy and spectroscopic imaging of {1-13C}-g1ucose and its metabolic products. Magnetic Resonance in Medicine, 1993, 30, 544-551.	3.0	98
22	Comparative study of ferrofluids based on dextran-coated iron oxide and metal nanoparticles for contrast agents in magnetic resonance imaging. Nanotechnology, 2004, 15, S154-S159.	2.6	88
23	A Modular Labeling Strategy for In Vivo PET and Near-Infrared Fluorescence Imaging of Nanoparticle Tumor Targeting. Journal of Nuclear Medicine, 2014, 55, 1706-1711.	5.0	85
24	AMPK Phosphorylation Modulates Pain by Activation of NLRP3 Inflammasome. Antioxidants and Redox Signaling, 2016, 24, 157-170.	5.4	85
25	Use of perfluorocarbon nanoparticles for nonâ€invasive multimodal cell tracking of human pancreatic islets. Contrast Media and Molecular Imaging, 2011, 6, 251-259.	0.8	83
26	Magnetoelectroporation: improved labeling of neural stem cells and leukocytes for cellular magnetic resonance imaging using a single FDA-approved agent. Nanomedicine: Nanotechnology, Biology, and Medicine, 2006, 2, 89-94.	3.3	81
27	A metabolomic approach for diagnosis of experimental sepsis. Intensive Care Medicine, 2011, 37, 2023-2032.	8.2	80
28	Tumor Necrosis Factor-α Increases the Steady-state Reduction of Cytochrome b of the Mitochondrial Respiratory Chain in Metabolically Inhibited L929 Cells. Journal of Biological Chemistry, 2000, 275, 13353-13361.	3.4	78
29	p38Î ³ is essential for cell cycle progression and liver tumorigenesis. Nature, 2019, 568, 557-560.	27.8	72
30	Fast synthesis and bioconjugation of ⁶⁸ Ga coreâ€doped extremely small iron oxide nanoparticles for PET/MR imaging. Contrast Media and Molecular Imaging, 2016, 11, 203-210.	0.8	68
31	Mealiness assessment in apples and peaches using MRI techniques. Magnetic Resonance Imaging, 2000, 18, 1175-1181.	1.8	66
32	Ablation of the stress protease OMA1 protects against heart failure in mice. Science Translational Medicine, 2018, 10, .	12.4	66
33	Regulation of Mother-to-Offspring Transmission of mtDNA Heteroplasmy. Cell Metabolism, 2019, 30, 1120-1130.e5.	16.2	66
34	The novel DNA methylation inhibitor zebularine is effective against the development of murine T-cell lymphoma. Blood, 2006, 107, 1174-1177.	1.4	64
35	Liver and brain imaging through dimercaptosuccinic acid-coated iron oxide nanoparticles. Nanomedicine, 2010, 5, 397-408.	3.3	64
36	β3 adrenergic receptor selective stimulation during ischemia/reperfusion improves cardiac function in translational models through inhibition of mPTP opening in cardiomyocytes. Basic Research in Cardiology, 2014, 109, 422.	5.9	63

#	Article	IF	CITATIONS
37	Hybrid Decorated Core@Shell Janus Nanoparticles as a Flexible Platform for Targeted Multimodal Molecular Bioimaging of Cancer. ACS Applied Materials & Interfaces, 2018, 10, 31032-31043.	8.0	61
38	Long-Term Dabigatran Treatment Delays Alzheimer's Disease Pathogenesis in the TgCRND8ÂMouse Model. Journal of the American College of Cardiology, 2019, 74, 1910-1923.	2.8	61
39	Effects of oxygen and glucose deprivation on the expression and distribution of neuronal and inducible nitric oxide synthases and on protein nitration in rat cerebral cortex. Journal of Comparative Neurology, 2002, 443, 183-200.	1.6	58
40	Cooperation between Cdk4 and p27kip1 in Tumor Development: A Preclinical Model to Evaluate Cell Cycle Inhibitors with Therapeutic Activity. Cancer Research, 2005, 65, 3846-3852.	0.9	55
41	Colloidal dispersions of maghemite nanoparticles produced by laser pyrolysis with application as NMR contrast agents. Journal Physics D: Applied Physics, 2004, 37, 2054-2059.	2.8	54
42	A novel R-package graphic user interface for the analysis of metabonomic profiles. BMC Bioinformatics, 2009, 10, 363.	2.6	54
43	MKK6 controls T3-mediated browning of white adipose tissue. Nature Communications, 2017, 8, 856.	12.8	54
44	NLRP3-inflammasome inhibition prevents high fat and high sugar diets-induced heart damage through autophagy induction. Oncotarget, 2017, 8, 99740-99756.	1.8	53
45	Descriptive review of current NMR-based metabolomic data analysis packages. Progress in Nuclear Magnetic Resonance Spectroscopy, 2011, 59, 263-270.	7.5	51
46	Vascular smooth muscle cellâ€specific progerin expression in a mouse model of Hutchinson–Gilford progeria syndrome promotes arterial stiffness: Therapeutic effect of dietary nitrite. Aging Cell, 2019, 18, e12936.	6.7	51
47	Tumor Necrosis Factor-α Increases ATP Content in Metabolically Inhibited L929 Cells Preceding Cell Death. Journal of Biological Chemistry, 1997, 272, 30167-30177.	3.4	49
48	Mealiness assessment in apples using MRI techniques. Magnetic Resonance Imaging, 1999, 17, 275-281.	1.8	47
49	Experimental methods for flow and aerosol measurements in human airways and their replicas. European Journal of Pharmaceutical Sciences, 2018, 113, 95-131.	4.0	46
50	Fingerprintingâ€based metabolomic approach with <scp>LC</scp> â€ <scp>MS</scp> to sleep apnea and hypopnea syndrome: A pilot study. Electrophoresis, 2013, 34, 2873-2881.	2.4	45
51	Metabolomics Reveals Metabolite Changes in Acute Pulmonary Embolism. Journal of Proteome Research, 2014, 13, 805-816.	3.7	45
52	Probiotic <i>Bifidobacterium breve</i> prevents DOCAâ€salt hypertension. FASEB Journal, 2020, 34, 13626-13640.	0.5	45
53	Iron Oxide Nanoparticles: An Alternative for Positive Contrast in Magnetic Resonance Imaging. Inorganics, 2020, 8, 28.	2.7	45
54	Gradient-enhanced heteronuclear correlation spectroscopy. Theory and experimental aspects. Journal of Magnetic Resonance, 1992, 100, 282-302.	0.5	44

#	Article	IF	CITATIONS
55	One-Step Fast Synthesis of Nanoparticles for MRI: Coating Chemistry as the Key Variable Determining Positive or Negative Contrast. Langmuir, 2017, 33, 10239-10247.	3.5	43
56	The application of nanoparticles in gene therapy and magnetic resonance imaging. Microscopy Research and Technique, 2011, 74, 577-591.	2.2	40
57	Non-destructive seed detection in mandarins: Comparison of automatic threshold methods in FLASH and COMSPIRA MRIs. Postharvest Biology and Technology, 2008, 47, 189-198.	6.0	39
58	Role of Peroxynitrite in Sepsis-Induced Acute Kidney Injury in an Experimental Model of Sepsis in Rats. Shock, 2012, 38, 403-410.	2.1	39
59	Parallel Multifunctionalization of Nanoparticles: A One-Step Modular Approach for in Vivo Imaging. Bioconjugate Chemistry, 2015, 26, 153-160.	3.6	39
60	In vivo imaging of lung inflammation with neutrophil-specific 68Ga nano-radiotracer. Scientific Reports, 2017, 7, 13242.	3.3	37
61	Family of Bioactive Heparin-Coated Iron Oxide Nanoparticles with Positive Contrast in Magnetic Resonance Imaging for Specific Biomedical Applications. Biomacromolecules, 2017, 18, 3156-3167.	5.4	37
62	In vivo diffusion weighted19F MRI using SF6. Magnetic Resonance in Medicine, 2005, 54, 460-463.	3.0	36
63	Could NLRP3–Inflammasome Be a Cardiovascular Risk Biomarker in Acute Myocardial Infarction Patients?. Antioxidants and Redox Signaling, 2017, 27, 269-275.	5.4	36
64	Quantification of water compartmentation in cell suspensions by diffusion-weighted and T2-weighted MRI. Magnetic Resonance Imaging, 2008, 26, 88-102.	1.8	35
65	Cu-Doped Extremely Small Iron Oxide Nanoparticles with Large Longitudinal Relaxivity: One-Pot Synthesis and in Vivo Targeted Molecular Imaging. ACS Omega, 2019, 4, 2719-2727.	3.5	35
66	Detection of freeze injury in oranges by magnetic resonance imaging of moving samples. Applied Magnetic Resonance, 2004, 26, 431-445.	1.2	34
67	Gene Silencing of SOCS3 by siRNA Intranasal Delivery Inhibits Asthma Phenotype in Mice. PLoS ONE, 2014, 9, e91996.	2.5	34
68	NLRP3 Inflammasome Inhibition by MCC950 in Aged Mice Improves Health via Enhanced Autophagy and PPARα Activity. Journals of Gerontology - Series A Biological Sciences and Medical Sciences, 2020, 75, 1457-1464.	3.6	33
69	A New Method for the Rapid Synthesis of Water Stable Superparamagnetic Nanoparticles. Chemistry - A European Journal, 2008, 14, 9126-9130.	3.3	32
70	New Biochemical Insights into the Mechanisms of Pulmonary Arterial Hypertension in Humans. PLoS ONE, 2016, 11, e0160505.	2.5	32
71	On-line Identification of Seeds in Mandarins with Magnetic Resonance Imaging. Biosystems Engineering, 2006, 95, 529-536.	4.3	31
72	Aerosols and gaseous contrast agents for magnetic resonance imaging of the lung. Contrast Media and Molecular Imaging, 2008, 3, 173-190.	0.8	31

#	Article	IF	CITATIONS
73	Cell identity and nucleo-mitochondrial genetic context modulate OXPHOS performance and determine somatic heteroplasmy dynamics. Science Advances, 2020, 6, eaba5345.	10.3	31
74	Metabolic Reprogramming in the Heart and Lung in a Murine Model of Pulmonary Arterial Hypertension. Frontiers in Cardiovascular Medicine, 2018, 5, 110.	2.4	30
75	Diffusion-weighted 19F-MRI of lung periphery: Influence of pressure and air–SF6 composition on apparent diffusion coefficients. Respiratory Physiology and Neurobiology, 2005, 148, 43-56.	1.6	27
76	Identification of novel metabolomic biomarkers in an experimental model of septic acute kidney injury. American Journal of Physiology - Renal Physiology, 2019, 316, F54-F62.	2.7	27
77	Human influenza A virus causes myocardial and cardiac-specific conduction system infections associated with early inflammation and premature death. Cardiovascular Research, 2021, 117, 876-889.	3.8	27
78	Changes in water status of cherimoya fruit during ripening. Postharvest Biology and Technology, 2007, 45, 147-150.	6.0	26
79	A new method for the aqueous functionalization of superparamagnetic Fe ₂ O ₃ nanoparticles. Contrast Media and Molecular Imaging, 2008, 3, 215-222.	0.8	26
80	Phosphatidylcholine oated Iron Oxide Nanomicelles for In Vivo Prolonged Circulation Time with an Antibiofouling Protein Corona. Chemistry - A European Journal, 2014, 20, 16662-16671.	3.3	26
81	Recent advances in the preparation and application of multifunctional iron oxide and liposome-based nanosystems for multimodal diagnosis and therapy. Interface Focus, 2016, 6, 20160055.	3.0	26
82	Noninvasive real-time monitoring of intracellular cancer cell metabolism and response to lonidamine treatment using diffusion weighted proton magnetic resonance spectroscopy. Cancer Research, 2000, 60, 5179-86.	0.9	26
83	Is NMR-based metabolomic analysis of exhaled breath condensate accurate?. European Respiratory Journal, 2011, 37, 468-470.	6.7	25
84	Superparamagnetic Nanoparticles for Atherosclerosis Imaging. Nanomaterials, 2014, 4, 408-438.	4.1	25
85	Discovery and validation of an NMR-based metabolomic profile in urine as TB biomarker. Scientific Reports, 2020, 10, 22317.	3.3	24
86	Computer-assisted enhanced volumetric segmentation magnetic resonance imaging data using a mixture of artificial neural networks. Magnetic Resonance Imaging, 2003, 21, 901-912.	1.8	23
87	Magnetosonoporation: Instant magnetic labeling of stem cells. Magnetic Resonance in Medicine, 2010, 63, 1437-1441.	3.0	23
88	Ultrasmall Manganese Ferrites for In Vivo Catalase Mimicking Activity and Multimodal Bioimaging. Small, 2022, 18, e2106570.	10.0	23
89	Automatic tuning and matching of a small multifrequency saddle coil at 4.7 T. Magnetic Resonance in Medicine, 2004, 51, 869-873.	3.0	22
90	Detection of seeds in citrus using MRI under motion conditions and improvement with motion correction. Concepts in Magnetic Resonance Part B, 2005, 26B, 81-92.	0.7	22

#	Article	IF	CITATIONS
91	Metabolomic Profile of ARDS by Nuclear Magnetic Resonance Spectroscopy in Patients With H1N1 Influenza Virus Pneumonia. Shock, 2018, 50, 504-510.	2.1	22
92	Interventional magnetic resonance imaging for guiding gene and cell transfer in the heart. British Heart Journal, 2004, 90, 87-91.	2.1	21
93	A Metabolomic Approach to the Pathogenesis of Ventilator-induced Lung Injury. Anesthesiology, 2014, 120, 694-702.	2.5	21
94	T1-MRI Fluorescent Iron Oxide Nanoparticles by Microwave Assisted Synthesis. Nanomaterials, 2015, 5, 1880-1890.	4.1	21
95	Reactive oxygen species mediate the down-regulation of mitochondrial transcripts and proteins by tumour necrosis factor-alpha in L929 cells. Biochemical Journal, 2003, 370, 609-619.	3.7	20
96	Cardiovascular imaging: what have we learned from animal models?. Frontiers in Pharmacology, 2015, 6, 227.	3.5	20
97	Metabolomic diferences between COVID-19 and H1N1 influenza induced ARDS. Critical Care, 2021, 25, 390.	5.8	20
98	HIV transgene expression impairs K ⁺ channel function in the pulmonary vasculature. American Journal of Physiology - Lung Cellular and Molecular Physiology, 2018, 315, L711-L723.	2.9	19
99	Blockade of the NLRP3 inflammasome improves metabolic health and lifespan in obese mice. GeroScience, 2020, 42, 715-725.	4.6	19
100	Effects of Colchicine on Atherosclerotic Plaque Stabilization: a Multimodality Imaging Study in an Animal Model. Journal of Cardiovascular Translational Research, 2021, 14, 150-160.	2.4	19
101	Molecular Imaging with 68Ga Radio-Nanomaterials: Shedding Light on Nanoparticles. Applied Sciences (Switzerland), 2018, 8, 1098.	2.5	18
102	Unambiguous detection of atherosclerosis using bioorthogonal nanomaterials. Nanomedicine: Nanotechnology, Biology, and Medicine, 2019, 17, 26-35.	3.3	18
103	MRI Visualization of Small Structures Using Improved Surface Coils. Magnetic Resonance Imaging, 1998, 16, 157-166.	1.8	17
104	Hormone dependence of breast cancer cells and the effects of tamoxifen and estrogen:31P NMR studies. Breast Cancer Research and Treatment, 1995, 33, 209-217.	2.5	16
105	A history of biological applications of NMR spectroscopy. Progress in Nuclear Magnetic Resonance Spectroscopy, 1995, 28, 53-85.	7.5	16
106	Microwave-driven synthesis of bisphosphonate nanoparticles allows in vivo visualisation of atherosclerotic plaque. RSC Advances, 2015, 5, 1661-1665.	3.6	16
107	Accurate quantification of atherosclerotic plaque volume by 3D vascular ultrasound using the volumetric linear array method. Atherosclerosis, 2016, 248, 230-237.	0.8	16
108	Chilling Temperature Storage Changes the Inorganic Phosphate Pool Distribution in Cherimoya (Annona cherimola) Fruit. Journal of the American Society for Horticultural Science, 2001, 126, 122-127.	1.0	16

#	Article	IF	CITATIONS
109	Magnetic resonance imaging in the evaluation of inflammatory lesions in muscular and soft tissues: an experimental infection model induced by Candida albicans. Magnetic Resonance Imaging, 1999, 17, 1327-1334.	1.8	15
110	Monitoring acute inflammatory processes in mouse muscle by MR imaging and spectroscopy: a comparison with pathological results. NMR in Biomedicine, 2002, 15, 204-214.	2.8	15
111	Magnetic Resonance Methods and Applications in Pharmaceutical Research. Journal of Pharmaceutical Sciences, 2008, 97, 3637-3665.	3.3	15
112	Iron Oxide Nanoradiomaterials: Combining Nanoscale Properties with Radioisotopes for Enhanced Molecular Imaging. Contrast Media and Molecular Imaging, 2017, 2017, 1-24.	0.8	15
113	Micellar Iron Oxide Nanoparticles Coated with Anti-Tumor Glycosides. Nanomaterials, 2018, 8, 567.	4.1	15
114	MicroRNA Nanotherapeutics for Lung Targeting. Insights into Pulmonary Hypertension. International Journal of Molecular Sciences, 2020, 21, 3253.	4.1	15
115	Increase in the ATP signal after treatment with cisplatin in two different cell lines studied by 31P NMR spectroscopy. Biochemical and Biophysical Research Communications, 1992, 183, 114-120.	2.1	14
116	Optimization of magnetosonoporation for stem cell labeling. NMR in Biomedicine, 2010, 23, 480-484.	2.8	14
117	Bmi1 limits dilated cardiomyopathy and heart failure by inhibiting cardiac senescence. Nature Communications, 2015, 6, 6473.	12.8	14
118	Experimental results of an evolution-based adaptation strategy for VQ image filtering. Information Sciences, 2001, 133, 249-266.	6.9	13
119	COMSPIRA: A common approach to spiral and radial MRI. , 2004, 20B, 40-44.		13
120	Gradient-enhanced heteronuclear correlation spectroscopy: Theory and experimental aspects. Journal of Magnetic Resonance, 2011, 213, 446-466.	2.1	13
121	Hybrid microparticles for drug delivery and magnetic resonance imaging. Journal of Biomedical Materials Research - Part B Applied Biomaterials, 2013, 101B, 498-505.	3.4	13
122	Systems medicine: A new approach to clinical practice. Archivos De Bronconeumologia, 2014, 50, 444-451.	0.8	13
123	Surfaceâ€Functionalized Nanoparticles by Olefin Metathesis: A Chemoselective Approach for In Vivo Characterization of Atherosclerosis Plaque. Chemistry - A European Journal, 2015, 21, 10450-10456.	3.3	13
124	MRI Study of the Influence of Surface Coating Aging on the In Vivo Biodistribution of Iron Oxide Nanoparticles. Biosensors, 2018, 8, 127.	4.7	13
125	Discriminant biomarkers of acute respiratory distress syndrome associated to H1N1 influenza identified by metabolomics HPLCâ€QTOFâ€MS/MS platform. Electrophoresis, 2017, 38, 2341-2348.	2.4	12
126	Protein corona and phospholipase activity drive selective accumulation of nanomicelles in atherosclerotic plaques. Nanomedicine: Nanotechnology, Biology, and Medicine, 2018, 14, 643-650.	3.3	12

#	Article	IF	CITATIONS
127	Fluorine Labeling of Nanoparticles and In Vivo ¹⁹ F Magnetic Resonance Imaging. ACS Applied Materials & Interfaces, 2021, 13, 12941-12949.	8.0	12
128	HAP-Multitag, a PET and Positive MRI Contrast Nanotracer for the Longitudinal Characterization of Vascular Calcifications in Atherosclerosis. ACS Applied Materials & Interfaces, 2021, 13, 45279-45290.	8.0	12
129	Measurement of Pharmacodynamic Effects of Dexamethasone on Epidermis by Phosphorus Nuclear Magnetic Resonance Spectroscopy in Vitro. Journal of Pharmaceutical Sciences, 1994, 83, 1339-1344.	3.3	11
130	Random Walk Simulation of the MRI Apparent Diffusion Coefficient in a Geometrical Model of the Acinar Tree. Biophysical Journal, 2009, 97, 656-664.	0.5	10
131	Metabolomic profile of acute respiratory distress syndrome of different etiologies. Intensive Care Medicine, 2019, 45, 1318-1320.	8.2	10
132	Activation of amino acid metabolic program in cardiac HIF1-alpha-deficient mice. IScience, 2021, 24, 102124.	4.1	10
133	Heteroplasmy of Wild-Type Mitochondrial DNA Variants in Mice Causes Metabolic Heart Disease With Pulmonary Hypertension and Frailty. Circulation, 2022, 145, 1084-1101.	1.6	10
134	Olefin metathesis for the functionalization of superparamagnetic nanoparticles. Bioinspired, Biomimetic and Nanobiomaterials, 2012, 1, 166-172.	0.9	9
135	Superparamagnetic iron oxide nanoparticles conjugated to a grass pollen allergen and an optical probe. Contrast Media and Molecular Imaging, 2012, 7, 435-439.	0.8	9
136	Medicina de sistemas: una nueva visión de la práctica clÃnica. Archivos De Bronconeumologia, 2014, 50, 444-451.	0.8	9
137	Effects of Quercetin in a Rat Model of Hemorrhagic Traumatic Shock and Reperfusion. Molecules, 2016, 21, 1739.	3.8	9
138	Aging and the Inflammasomes. Experientia Supplementum (2012), 2018, 108, 303-320.	0.9	9
139	Thrombo-tag, an <i>in vivo</i> formed nanotracer for the detection of thrombi in mice by fast pre-targeted molecular imaging. Nanoscale, 2020, 12, 22978-22987.	5.6	9
140	Urine NMR-based TB metabolic fingerprinting for the diagnosis of TB in children. Scientific Reports, 2021, 11, 12006.	3.3	9
141	Delayed alveolar clearance of nanoparticles through control of coating composition and interaction with lung surfactant protein A. Materials Science and Engineering C, 2022, 134, 112551.	7.3	9
142	NMR and the Study of Pathological State in Cells and Tissues. International Review of Cytology, 1993, 145, 1-63.	6.2	8
143	Interaction of Bovine Myelin Basic Protein with Cholesterol. Journal of Colloid and Interface Science, 1998, 204, 9-15.	9.4	8
144	A metabonomic approach to evaluate COPD in a model of cigarette smoke exposure in mice. Metabolomics, 2010, 6, 564-573.	3.0	8

#	Article	IF	CITATIONS
145	Heparin length in the coating of extremely small iron oxide nanoparticles regulates <i>in vivo</i> theranostic applications. Nanoscale, 2021, 13, 842-861.	5.6	8
146	The thermal transition in crude myelin proteolipid has a lipid rather than protein origin. European Biophysics Journal, 1992, 21, 71-6.	2.2	7
147	Gradient-enhanced multiple-quantum filter (ge-MQF). A simple way to obtain single-scan phase-sensitive HMQC spectra. Journal of Magnetic Resonance, 1992, 100, 215-220.	0.5	7
148	Magnetic resonance microscopy versus light microscopy in human embryology teaching. Clinical Anatomy, 2004, 17, 429-435.	2.7	7
149	The acid metabolism ofAnnonafruit during ripening. Journal of Horticultural Science and Biotechnology, 2004, 79, 472-478.	1.9	7
150	Longâ€range diffusion of hyperpolarized ³ He in rats. Magnetic Resonance in Medicine, 2009, 61, 54-58.	3.0	7
151	Assessment of regional pulmonary blood flow using 68Ga-DOTA PET. EJNMMI Research, 2017, 7, 7.	2.5	7
152	The State of the Art of Investigational and Approved Nanomedicine Products for Nucleic Acid Delivery. , 2019, , 421-456.		7
153	A dual 1H/19F birdcage coil for small animals at 7ÂT MRI. Magnetic Resonance Materials in Physics, Biology, and Medicine, 2019, 32, 79-87.	2.0	7
154	Plasma Metabolic Signature of Atherosclerosis Progression and Colchicine Treatment in Rabbits. Scientific Reports, 2020, 10, 7072.	3.3	7
155	Thermal stability of bovine-brain myelin membrane. European Biophysics Journal, 1992, 21, 169-78.	2.2	6
156	Changes in ATP after cyclosporin A treatment in a renal epithelial cell line in the rat studied by 31P-NMR spectroscopy. Research Communications in Molecular Pathology and Pharmacology, 1994, 86, 3-13.	0.2	6
157	In vitro cytotoxic effects of tumor necrosis factor-α in human breast cancer cells may be associated with increased glucose consumption. FEBS Letters, 1997, 406, 175-178.	2.8	5
158	A fully MRI-compatible animal ventilator for special-gas mixing applications. Concepts in Magnetic Resonance Part B, 2005, 26B, 93-103.	0.7	5
159	A MRI and Polarized Gases Compatible Respirator and Gas Administrator for the Study of the Small Animal Lung: Volume Measurement and Control. IEEE Transactions on Biomedical Engineering, 2010, 57, 1745-1749.	4.2	5
160	Dynamic Ventilation \$^3\$He MRI for the Quantification of Disease in the Rat Lung. IEEE Transactions on Biomedical Engineering, 2012, 59, 777-786.	4.2	5
161	Lung Tissue Volume is Elevated in Obesity and Reduced by Bariatric Surgery. Obesity Surgery, 2016, 26, 2475-2482.	2.1	5
162	Digitonin concentration is determinant for mitochondrial supercomplexes analysis by BlueNative page. Biochimica Et Biophysica Acta - Bioenergetics, 2021, 1862, 148332.	1.0	5

#	Article	IF	CITATIONS
163	Probe efficiency improvement with remote and transmission line tuning and matching. Magnetic Resonance Imaging, 1999, 17, 1083-1086.	1.8	4
164	Density matrix calculations in Mathematica?. Concepts in Magnetic Resonance, 2001, 13, 143-147.	1.3	4
165	Quantitative assessment of myocardial blood flow and extracellular volume fraction using 68Ga-DOTA-PET: A feasibility and validation study in large animals. Journal of Nuclear Cardiology, 2020, 27, 1249-1260.	2.1	4
166	In Vivo 18F-FDG-PET Imaging in Mouse Atherosclerosis. Methods in Molecular Biology, 2015, 1339, 377-386.	0.9	4
167	Magnetic Resonance Imaging of the Atherosclerotic Mouse Aorta. Methods in Molecular Biology, 2015, 1339, 387-394.	0.9	4
168	Effects of Ethanol and Dexamethasone on Epidermis Examined by in Vitro 31P Magnetic Resonance Spectroscopy. Journal of Pharmaceutical Sciences, 1998, 87, 249-255.	3.3	3
169	VQ based Bayesian image filtering. , 2000, , .		3
170	Influence of ambient air on NMR-based metabolomics of exhaled breath condensates. European Respiratory Journal, 2012, 40, 1294-1296.	6.7	3
171	Covalent functionalization of magnetic nanoparticles for biomedical imaging. SPIE Newsroom, 0, , .	0.1	3
172	Apparent diffusion coefficient of hyperpolarized ³ He with minimal influence of the residual gas in small animals. NMR in Biomedicine, 2012, 25, 1026-1032.	2.8	3
173	Synthesis of ⁶⁸ Ga Core-doped Iron Oxide Nanoparticles for Dual Positron Emission Tomography /(T ₁)Magnetic Resonance Imaging. Journal of Visualized Experiments, 2018, , .	0.3	3
174	Benchtop nuclear magnetic resonanceâ€based metabolomic approach for the diagnosis of bovine tuberculosis. Transboundary and Emerging Diseases, 2022, 69, .	3.0	3
175	Pathway selection by pulsed field gradients. Magnetic Resonance in Medicine, 2002, 48, 540-542.	3.0	2
176	Magnetic resonance spectrometer controller and data postprocessing software. , 2003, 16B, 1-14.		2
177	COMSPIRA3D: A combined approach to radial and spiral 3D MRI. Concepts in Magnetic Resonance Part B, 2006, 29B, 115-124.	0.7	2
178	Iron Oxide Nanoparticle-Based MRI Contrast Agents: Characterization and In Vivo Use. , 2017, , 85-120.		2
179	Engineered polymeric nanovehicles for drug delivery. Frontiers of Nanoscience, 2020, 16, 201-232.	0.6	2
180	Improvement of functional magnetic resonance images by pretreatment of data. European Biophysics Journal, 1996, 24, 335-41.	2.2	1

#	Article	IF	CITATIONS
181	MRI texture analysis as means for addressing rehydration and milk diffusion in cereals. Procedia Food Science, 2011, 1, 625-631.	0.6	1
182	Microwave-driven Synthesis of Iron Oxide Nanoparticles for Fast Detection of Atherosclerosis. Journal of Visualized Experiments, 2016, , .	0.3	1
183	Assessing the Potential of Molecular Imaging for Myelin Quantification in Organotypic Cultures. Pharmaceutics, 2021, 13, 975.	4.5	1
184	In-vivo lung molecular imaging of choline metabolism in a rat model of pulmonary arterial hypertension. , 2019, , .		1
185	Inflamm-ageing or inflammasom-ageing as independent events. Aging, 2020, 12, 17759-17760.	3.1	1
186	High resolution in vivo imaging at high frequencies with improved surface coils. , 0, , .		0
187	Segmentation of infected tissues in MRI based on VQ-BF filtering. , 0, , .		0
188	On a Gradient-based Evolution Strategy for Parametric Illumination Correction. , 2005, , 61-72.		0
189	CMR 2007: 11.01: PFOB trimodal microcapsules for immunoprotection and visualization of cellular therapeutics with ultrasound, CT and MRI. Contrast Media and Molecular Imaging, 2007, 2, 297-298.	0.8	0
190	New Murine Sub-massive Pulmonary Embolism Model, Sensitive To Both Clinical Treatments And Diagnostic Techniques. , 2010, , .		0
191	Efecto de la segmentación por tejidos en los mapas de atenuación sobre la cuantificación PET con especial hincapié en grandes arterias. Revista Espanola De Medicina Nuclear E Imagen Molecular, 2018, 37, 94-102.	0.0	0
192	MODELLING PHASE-SHIFT FOR MOTION CORRECTION IN MRI ON-LINE APPLICATIONS. Acta Horticulturae, 2005, , 173-179.	0.2	0
193	MODELING FOR METABONOMIC FINGERPRINT ASSIGNMENT IN OLIVE FRUITS. Acta Horticulturae, 2008, , 393-400.	0.2	0
194	Uniform Magnetite Nanoparticles Larger Than 20 nm Synthesized by an Aqueous Route. Springer Proceedings in Physics, 2012, , 379-379.	0.2	0
195	Can the lung be obese? Lung tissue volume (<i>Vtiss</i>) is elevated in severe obesity and reduced by bariatric surgery. , 2016, , .		0
196	Benchtop NMR-based metabolomic analysis as a diagnostic tool for tuberculosis in clinical urine samples. , 2019, , .		0
197	Detection of metabolic profile in urine for diagnosing pediatric tuberculosis. , 2019, , .		0
198	31P Nuclear Magnetic Resonance Spectroscopy of Cells and Tissues. Phosphorus, Sulfur and Silicon and the Related Elements, 1996, 109, 361-364.	1.6	0